

EMT Model of the ‘Sen Transformer’ for Fault Analysis Studies

Donald Fentie, Juan Carlos Garcia, Rama Gokaraju, Sherif Omar Faried

Abstract—The ‘Sen Transformer’ (ST) contains a number of tapped, magnetically-coupled, series transformer windings that provide independent active and reactive power flow control in a transmission line similar to a Unified UPFC. A transient model of the ST, using a hybrid transformer modeling approach is described in this paper. This model uses a non-linear core model (including saturation effects and losses), mutual coupling, zero sequence effects (to analyze unbalanced faults). Simulations are performed with PSCAD/EMTDC™. A Finite Element Analysis (FEA) model is also created for the ST using Flux 2D software. There is a good agreement between the two models in a test system for different types of fault scenarios.

Index Terms — Flexible AC Transmission Systems (FACTS), Power System Simulations, Power System Faults.

I. INTRODUCTION

MANY different Flexible AC Transmission Systems (FACTS) devices have been studied in the literature in order to control the flow of power through transmission lines. The Sen Transformer (ST) proposed in the research literature [1] uses transformer technology to independently control the active and reactive power in a transmission line.

In this paper, a transient model for the ST is described in PSCAD/EMTDC using a “hybrid” transformer modeling approach. This technique includes the non-linearities of the core, including losses and saturation effects, as well as inter-phase coupling, and zero sequence effects [2, 3]. The hybrid ST model can be used in power system studies such as transient and dynamic simulations, protection analysis. Fault analysis studies are presented in this paper.

A Finite Element Analysis (FEA) model is also created with Flux 2D software for comparison with the hybrid ST model. This method includes material non-linearities, and coupled electric circuits to obtain a precise transient solution for the ST. There is good agreement between the two models in a test system for multiple types of fault scenarios.

This paper is from the MSc thesis work of D. Fentie. The research was supported by the NSERC Industrial Postgraduate Scholarship of D. Fentie. D. Fentie, R. Gokaraju, S.O. Faried are with the University of Saskatchewan, Saskatoon, Canada. Emails: don.fentie@gmail.com, rama.krishna@usask.ca, sof280@mail.usask.ca.

J.C. Garcia is with the Manitoba HVDC Research Centre (a division of Manitoba Hydro International Ltd.), Winnipeg, Canada. Email: jcgzipa@mhi.ca

Paper submitted to the International Conference on Power Systems Transients (IPST2015) in Cavtat, Croatia June 15-18, 2015

A brief discussion about the ST is provided in Section II. Section III discusses the hybrid transformer modeling method including a core model, and leakage reactances. Section IV briefly describes the FEA model. Section V briefly gives the simulation results for few fault scenarios and Section VI discusses the conclusions.

II. SEN TRANSFORMER BACKGROUND

The “Sen” Transformer (ST) controls the flow of active and reactive power in transmission lines similar to a UPFC using transformer technology [1, 4]. The ST uses between 2 and 3 uniquely coupled series windings per phase. Taps located on the series windings are varied in order to arrive at a desired injected voltage magnitude and angle [4-6]. Tap changer technology typically operates in 1-2 seconds, which is adequate for most Utility power flow control applications [5]. In the system of Fig. 1 (a), the sending and receiving ends of a transmission line are separated by a line reactance, X , and an ST. The sending-end voltage, $V_s \angle \delta_s$, is modified by an ST compensating voltage, $V_{s/s} \angle \delta_{s/s}$, to create a new sending-end voltage, $V_{s'} \angle \delta_{s'}$. The receiving-end voltage, $V_r \angle \delta_r$, remains fixed as $V_r \angle \delta_r$ is varied. The ST compensating voltage $V_{s/s} \angle \delta_{s/s}$ is comprised of voltages V_d and V_q that are in phase and in quadrature with the incoming current I respectively. As a result, the ST exchanges active and reactive power, $P_{exchange}$ and $Q_{exchange}$, with the system. The receiving-end active and reactive power, P_r and Q_r , follow (1) and (2) [7]. Fig. 1 (b) depicts the phasor diagram of this system.

$$P_r = \frac{|V_{s'}||V_r|}{X} \sin(\delta_{s'} - \delta_r) \quad (1)$$

$$Q_r = \frac{|V_r|}{X} (|V_{s'}| \cos(\delta_{s'} - \delta_r) - |V_r|) \quad (2)$$

The compensating voltage $V_{s/s} \angle \delta_{s/s}$ can be modified within the limits of the ST, shown as the dashed circle in Fig. 1 (b), and at an angle β from 0° to 360° [5]. The voltage drop across the line reactance is shown as $V_x \angle \delta_x$. By creating the new sending-end voltage $V_{s'} \angle \delta_{s'}$, the active and reactive power flow can be controlled.

The ST contains an exciting unit and voltage regulating unit similar to a Phase Angle Regulator (PAR) in order to regulate the input voltage, V_{sa} to some desirable output voltage, $V_{s'a}$, in a transmission line. This regulation of voltage can be achieved with three series windings in the voltage regulation unit that are each magnetically coupled with a different exciting unit [1, 4]. The voltages injected by the series windings are separated by 120° and their magnitudes are controlled by a series of taps. Figure 2 shows the phase A connections of the ST for a three series winding configuration.

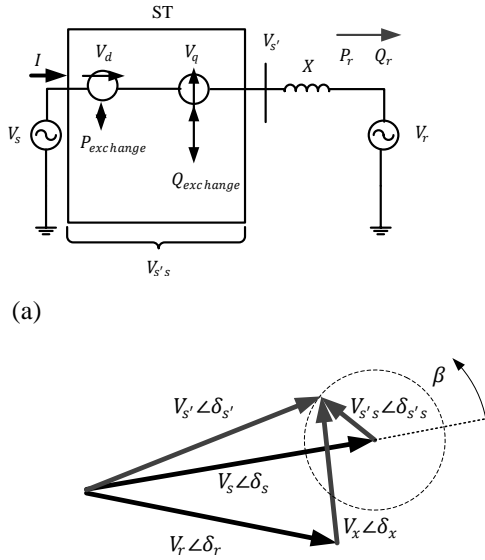


Fig. 1. (a) ST Power Flow Exchange. (b) ST Phasor Diagram.

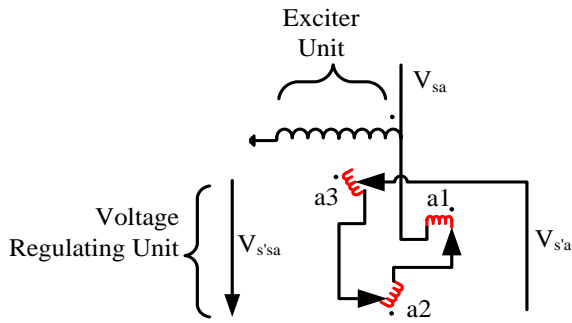


Fig. 2. Phase A of a three series winding ST.

Similarly, phases B and C would have series windings a2, b2, c2, and a3, b3, c3 respectively as well as excitation windings. All series windings are coupled to the same phase, such as a1, a2, and a3, must be tapped identically for symmetric operation. The construction view of a ST is shown in Fig. 3 [1].

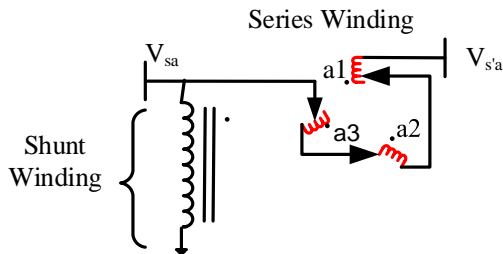


Fig. 3 Construction view of a ST.

The active and reactive power can be measured at the receiving-end of the line. Changing the tap position on each series winding modifies the power output and by modifying these taps over the entire voltage regulation range, β , of 360° a power 'envelope' can be formed. This envelope depicts the maximum change in power that the ST can achieve at a

particular angle of β . The active and reactive power envelopes are shown in Fig. 4 for the hybrid ST model comprising of three-winding transformers.

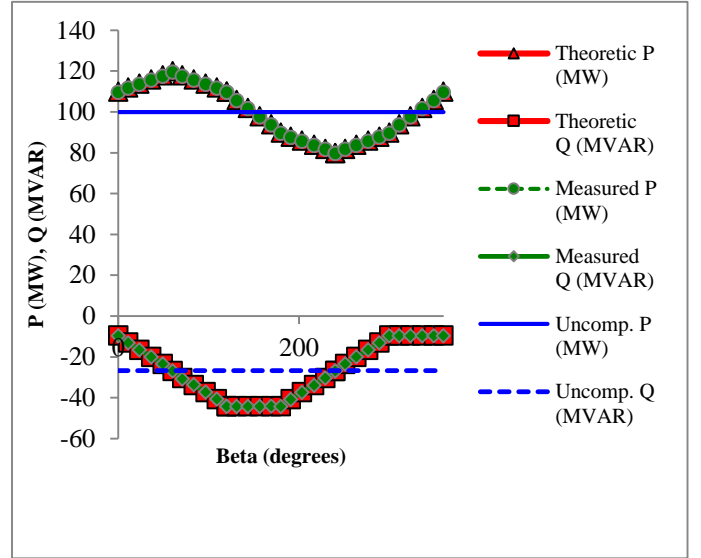


Fig. 4. Active and reactive power variation over voltage regulation range

Maximum active power transfer is achieved in the region of 0° to 120° and only two series windings are needed to operate in this region of the power envelope [4]. The results presented in this paper are based on a two series winding configuration as shown in Fig. 5.

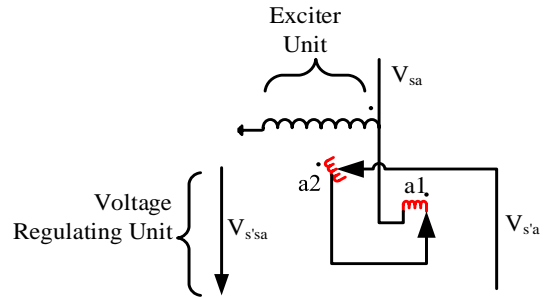


Fig. 5. Two series winding ST.

III. HYBRID ST MODEL

The model used is the hybrid transformer model [2, 9], which has been adapted for the purpose of simulating fault scenarios in an ST. The model can take into account individual saturation effects in the limbs of the core, magnetic coupling, leakage effects, non-linear core loss effects, and also coil resistances and capacitive interactions, if required. The hybrid model for a three-leg core is developed in PSCAD/EMDTC x4 interfaced with FORTRAN code. Figure 5 depicts the magnetic equivalent circuit of a 3-leg core (assuming all flux remains in the core). There are a total of 5 reluctances: 3 for the legs \mathcal{R}_a , \mathcal{R}_b , and \mathcal{R}_c and 2 for the yokes \mathcal{R}_1 and \mathcal{R}_2 . The winding-produced magnetomotive forces (mmfs) include \mathcal{F}_a' , \mathcal{F}_b' , and \mathcal{F}_c' . The flux ϕ in each component of Fig. 6 is identified with the same subscript as the reluctance that it flows through [8].

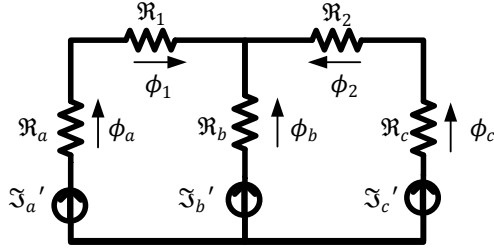


Fig. 6. Magnetic representation of 3-leg core.

An electric equivalent can be created as shown in Fig. 7 (a). The zero sequence flux paths are included in the electric equivalent core with zero-sequence impedance as shown in Fig. 7 (b).

The voltage sources E_A , E_B , and E_C are connected directly to a fictitious “ $m+1$ ” winding (to account for leakage flux linked by winding and not flowing in the core [2]), where m represents the number of physical transformer windings, on each phase of the transformer model. Core losses, zero sequence effects, and non-linear core effects are taken into account in this core. The rectangular units in Fig. 7 represent the core impedance of the legs, yokes, and zero-sequence flux paths. Each unit can be replaced with a branch that is appropriate for the study to be performed. All branches labeled Z_0 are zero sequence impedances between the tank and the core [2].

For the purposes of developing a model for faulted scenarios, a simplified branch approach of Fig. 8 is adopted where R_{EH} is the lumped eddy current and hysteresis losses and L_{sat} is the linear piecewise saturation curve.

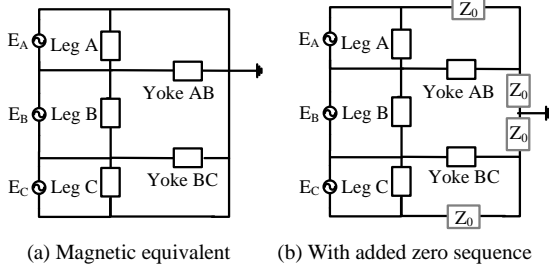


Fig. 7. Topological electric core equivalent.

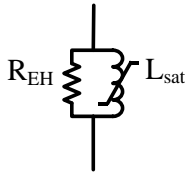


Fig. 8. Simplified branch representation for fault analysis.

A. Core Parameters – Resistance

The losses in Watts at 100% voltage can usually be obtained from transformer test reports and this allows core losses to be approximated as linear, which is good enough for most studies [9]. Swift [10] has shown that for transient analysis, eddy current losses are greater than hysteresis losses and can be approximated as a linear resistance. If the losses and exciting

current are provided at multiple voltage levels, it is possible to obtain a better estimation of the non-linear losses [11].

B. Core Parameters – Non-Linear Inductance

The non-linear inductance is simulated in PSCAD/EMTDC X4 using a modified saturable reactor that accepts voltage and current, flux linkage and current, or $B - H$ data. The $B - H$ curve for Armco M4 Steel was used with manufacturer data [12].

TABLE I
ARMCO M4 STEEL $B - H$ POINTS

B (T)	H (At/m)	B (T)	H (At/m)
0	0	1.4	23
0.6	6	1.6	55
0.8	8.4	1.7	130
1	11.1	1.8	416
1.2	14.4	1.9	1212

The $B - H$ curve is used as a linear piecewise approximation as shown in Fig. 9, which is the actual curve plotted from a saturable reactor in the core of the model used in this paper. It can accept up to 10 slopes to approximate the saturation curve and is a vast improvement over the two-slope classical approximation approaches.

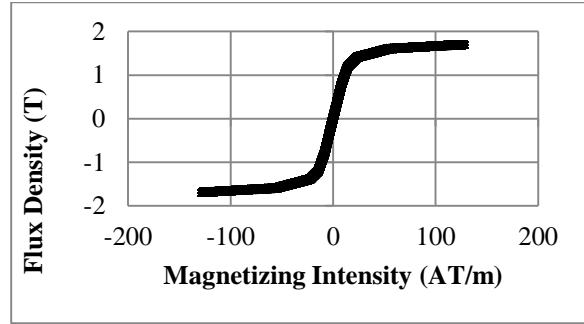


Fig. 9. Simulated Linear Piecewise B-H curve of Saturable Reactor.

C. Admittance Matrix Y

This matrix contains $(m+1)$ windings per phase where m is the total number of physical windings per phase for the transformer. In the case of a three-winding transformer with high, medium and low voltage windings (H , M , and L respectively), the Y matrix is shown in (21). Notice the extra row and column added for the core winding, C . The construction of the Y matrix for electromagnetic simulations is described in [13].

$$Y = \begin{bmatrix} Y_{11} & Y_{12} & Y_{13} & Y_{14} \\ Y_{21} & Y_{22} & Y_{23} & Y_{24} \\ Y_{31} & Y_{32} & Y_{33} & Y_{34} \\ Y_{41} & Y_{42} & Y_{43} & Y_{44} \end{bmatrix} \quad (21)$$

Since the magnetizing current, core losses, phase to phase coupling, flux interactions, zero-sequence effect, and saturation are all taken into account in the hybrid model core, the Y matrix can be constructed entirely with the leakage reactance information between windings. Short circuit tests can be

performed to determine the leakage reactance between all physical windings and those windings involving the core winding can be estimated.

Given a core that contains three windings, the leakage reactances between them can be represented as X_{HL} , X_{HM} , and X_{ML} where L=inner winding, M=middle winding, and H=outer winding. The “ $m+1$ ” winding is assumed to be located at the surface of the core and its reactance, X_C , is denoted with subscript ‘C’. The ratio of the leakage channels of the inner most and outer/middle most windings is defined as constant K [2], [14]. Since K changes based on design considerations that are likely only available to the transformer manufacturer, a value of $K = 0.5$ is a reasonable assumption [14]. The leakage reactance between windings and the core can be approximated [14] as:

$$X_{LC} \approx KX_{ML} \quad (22)$$

$$X_{MC} \approx (K + 1)X_{ML} \quad (23)$$

$$X_{HC} \approx X_{MC} + X_{HM}. \quad (24)$$

The admittance matrix handles the winding short circuit impedances and extra elements, such as a capacitive matrix and frequency dependent impedance windings, can also be added to the model, if required. It was found that the winding resistances have very negligible effect on the fault analysis studies and therefore are not taken into consideration and only the core model and inductance matrix are used. The extra resistance components can be added to the model easily, if needed in the studies.

IV. FINITE ELEMENT ANALYSIS ST MODEL

Finite Element Analysis (FEA) [15][16][17] using Flux 2D software is used for verifying the accuracy of the hybrid ST model. Only two-dimensional model is used in this paper due to the symmetry of the problem and no kinematics are required.

A three-leg ST is modeled using the Flux 2D software. The Dirichlet boundary around the problem is set based on initial tests. The majority of the flux flows in the transformer core during unsaturated conditions and the boundary does not need to be made excessively large. During times of saturation, most of the flux leaks relatively close around the windings through the air. The height, width, and area of the legs, the width and area of the yoke and the winding height are taken from a schematic drawing of a typical 100 MVA three-leg core transformer. The other core parameters were not released, however Cho [11] provides typical three-leg dimension ratios that are used to satisfy the yoke length dimension. Table II contains the geometry data of the transformer core and windings used for the FEA ST model. Short circuit tests are conducted to find the leakage reactances between the physical windings and the values are given in Table IV.

Each region in the physical geometry must be defined in the FEA model. The surrounding region around the core is classified as air. The winding regions are defined as conductor coils and must be oriented properly with respect to the coupled electric circuit. The magnetic material of the core is defined as Armco M4 Steel as shown in Table I. The windings are configured as coil regions and all other regions are defined as air.

TABLE II
FEA ST MODEL PARAMETERS

Parameter	Value
Yoke Length (m)	5.25
Yoke Width (m)	0.648
Yoke Area (m ²)	0.42
Leg Height (m)	3.046
Leg Width (m)	0.648
Leg Area (m ²)	0.42
Winding Height (m)	1.5
Dirichlet Boundary Length (m)	10
Outer Winding Width (mm)	120
Middle Winding Width (mm)	80
Inner Winding Width (mm)	80
Core to Inner Winding (mm)	45
Inner to Middle Winding (mm)	50
Middle to Outer Winding (mm)	60

Details of the nodes and mesh structure of this model are shown in Table III. The FEA model is coupled to the electric circuit shown in Fig. 10. The shunt and series windings in the figure refer to windings shown in the construction view provided for ST in Fig. 3 [1].

The sending-end source and impedance, V_S and Z_S respectively, and the receiving-end source and impedance, V_R and Z_R , are separated by an ST and line reactance X . The shunt winding and series windings are represented here as rectangular elements for simplicity but they follow the schematic of Figs. 2 and 3. The fault and fault impedance, Z_F , is shown between the series windings and transmission line. The shunt winding and series windings are represented here as rectangular elements for simplicity. This particular model uses a two-series-winding design in the voltage regulation domain $0^\circ \leq \beta \leq 120^\circ$, which allows for maximum power transfer over a transmission line. Circuit and FEA model parameters are shown in Table IV. Parameters involving the shunt winding are denoted with the subscript “1”, and the series windings are denoted with subscripts “2” and “3”. The leakage reactances labeled with a subscript “4” denote the calculated values for the fictitious core winding that will be used when the hybrid and FEA models are compared. The winding short circuit impedances to the core are calculated with (22)-(24) and the proportionality constant, K , is assumed to be 0.5.

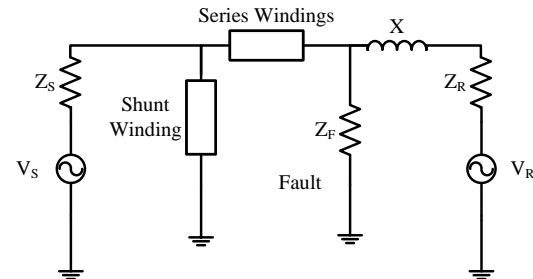


Fig 10. Single line diagram of the test circuit

V. RESULTS

The hybrid and FEA ST models are compared in this section for different fault types. The test setup parameters are shown in Table IV and the core material is given as M4 Armco steel whose B-H curve is shown in Table I. Core geometry is given in Table II, and the single line diagram of the test circuit is shown in Fig. 10.

TABLE III
FEA ST MODEL NODE DETAILS

Parameter	Value
Node Total	24977
Surface Elements	12472
Line Elements	1814
Large Node Spacing (mm)	1300
Medium Node Spacing (mm)	100
Small Node Spacing (mm)	40

A. Steady-State Normal Operation Results

The hybrid ST model is first compared to the FEA model under normal steady-state operation. The current is measured from the sending-end source side in each model. At normal operation the comparison between the two models is almost identical as shown in Fig. 11. The current is sinusoidal as expected with no asymmetrical offset.

TABLE IV
MODEL PARAMETERS FOR ST AND FEA COMPARISON

Parameter	Value
Phase	a-b-c
MVA	100
Winding 1 (kV _{L-L})	230
Winding 2-4 (kV _{L-L})	23
X ₁₂ (p.u.)	0.0438
X ₁₃ (p.u.)	0.0877
X ₂₃ (p.u.)	0.0365
X ₃₄ (p.u.)	0.01825
X ₂₄ (p.u.)	0.05475
X ₁₄ (p.u.)	0.09855
Fault Impedance, Z _F (Ω)	0.01
Series Winding Turns	70
Shunt Winding Turns	698
Source Impedances (p.u.)	0.00713+0.0428j
V _s (kV _{L-L})	230 ∠ 30°
V _r (kV _{L-L})	230 ∠ 0°
X (p.u.)	0.5

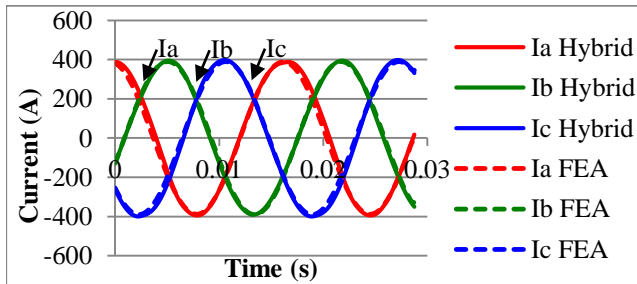


Fig 11. ST steady state normal operation current

B. Steady State Results

The steady state results of a three-phase, line-ground, and line-line fault are each obtained for both models and compared in Fig. 12. For each fault type, the results between both models are almost exactly identical with the resulting waveforms appearing on top of each other. The currents are sinusoidal with no offset, as expected, and separated electrically by 120°.

In all steady state tests of normal operation as well as three-phase, line-ground and line-line faults, the line currents for each phase is nearly identical between the hybrid ST model and the FEA ST model. These tests show that the hybrid ST model yields excellent steady state results for a variety of fault currents and it is an important step in proving the accuracy of the model for designing a protection scheme for the device. For true fault analysis however, it is necessary to view the fault transient current response in order to see the asymmetrical offset factor and offset decay. This transient portion of the model verification is examined in the next section.

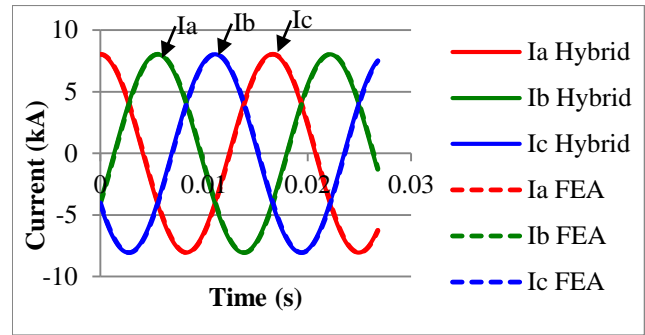


Fig 12 a). Three-phase steady state fault current

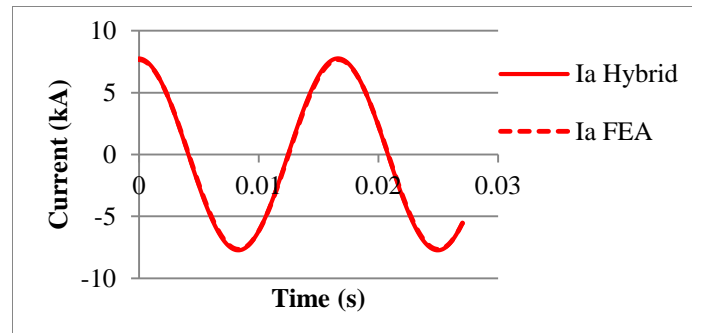


Fig 12 b). Line-ground steady state fault current

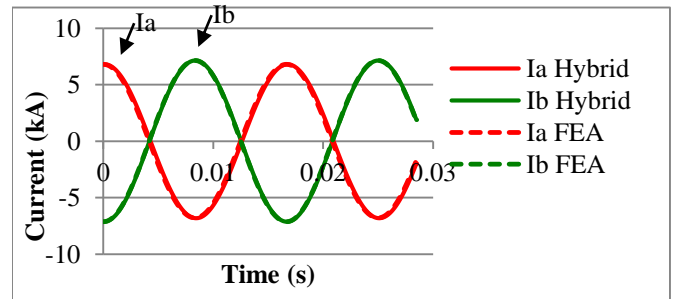


Fig 12 c). Line-line steady state fault current

C. Transient Results

The transient fault test comparisons between the FEA and hybrid ST models are the most important tests to show the accuracy of the hybrid model for fault analysis. The same test system and setup is used for both models as was used for the steady state analysis. For the FEA analysis, the time-variant modified version of Maxwell's law based on Ampère's circuital law is used [18].

The system is allowed to reach steady state after initial startup and a fault is applied at 0.5 seconds. The fault current results for three-phase, line-ground, and line-line faults are shown in Fig. 13 for the hybrid ST and FEA ST models.

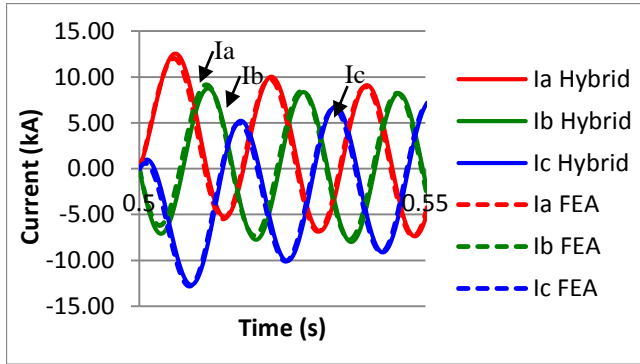


Fig 13 a). Three-phase transient fault current

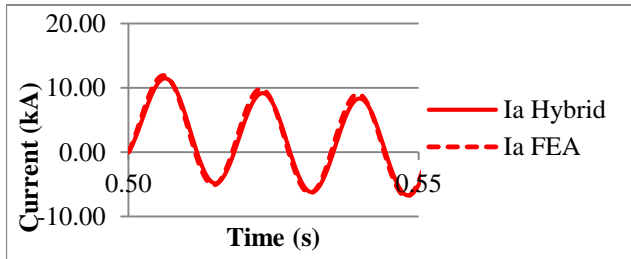


Fig 13 b). Line-ground transient fault current

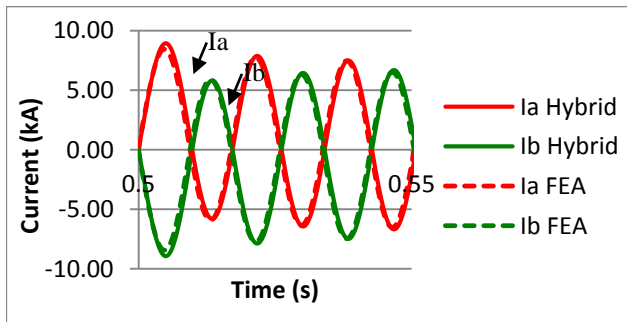


Fig 13 c). Line-line transient fault current

The comparison between the two methods for transient fault currents shows an excellent agreement between the two models. The maximum difference shown between the two models generally occurs in the peak of the first cycle and then the error is further reduced as the asymmetrical offset decays. The

maximum current error at the first peak in phase A after a fault is compared in Table V.

TABLE V
FEA VS. HYBRID ST: PEAK CURRENT COMPARISON

Transient Fault Type	Phase A Peak Current Following Fault (kA)		Percent Difference (%)
	FEA Model	Hybrid Model	
Three-phase	12.028	12.536	4.22
Line-ground	11.903	11.481	3.55
Line-line	8.408	8.933	6.24

From Table V, the maximum percent differences that occurred in the transient fault conditions were all around 5 percent. This is a very positive result especially considering the approximated lumped parameters used in the hybrid model core versus the much more accurate differential equations used to solve each meshed node in the FEA model. The symmetrical flux density as reported in the FEA model and hybrid model is given in Table VI.

In general, the percent differences between symmetric flux densities given in Table VI are less than 10% with the exception of the core leg that contains the faulted phase during a line-ground fault. The flux density in the core of the FEA ST model can have considerable variation throughout each leg and yoke due to the flux leakage, fringing effects, and non-linear properties of the magnetic material. As a result of this variation, the flux densities are taken in the geometric center of each core section of the FEA ST model. By contrast, the hybrid ST model assumes a constant flux density through a given leg or yoke due to the lumped nature of the components. This can explain some of the variation in the results shown.

In the faulted phase of the line-ground fault, there was a larger difference between the two models of measured flux density. It was found that the flux density in this leg varied a great deal if the zero sequence impedance was modified. The FEA model does not contain the transformer tank, which would directly affect the zero sequence impedance of the model. As a topic of future work, a tank could be constructed in the FEA model and the zero sequence impedance could be measured and emulated in the hybrid model to see how the two models compare.

VI. CONCLUSIONS

In this paper, a transient ST model was developed using the hybrid transformer modeling technique. The hybrid ST model was compared with the FEA ST model. The current and flux comparison results were found to be quite good between the two models for both steady state and transient faults.

The ST model is currently being developed for controlling active and reactive power flows in a transmission network using PSS/E software and the applications studies would be reported when the studies are completed.

VII. ACKNOWLEDGEMENTS

The authors thank Dr. Kalyan Sen, Sen Engineering Solutions, Pittsburgh, U.S.A. for the discussions on the M.Sc. thesis work of Mr. D. Fentie. The authors also thank the HVDC Research Centre for hosting Donald Fentie to carry the initial part of the modeling work at the HVDC Research Centre.

TABLE VI
FEA VS. HYBRID ST: PEAK SYMMETRIC FLUX DENSITY COMPARISON

Fault	Ph A Flux Density (T)		% Diff.	Phase B Flux Density (T)		% Diff.	Phase C Flux Density (T)		% Diff.
	FEA	Hyb		FEA	Hyb		FEA	Hyb	
	3-ph	0.27	0.25	9.4	0.27	0.25	8.96	0.27	0.255
L-G	0.31	0.27	13.1	1.61	1.63	1.74	1.71	1.742	1.87
L-L	0.97	0.97	0.10	0.71	0.70	0.99	1.61	1.629	0.87

VIII REFERENCES

- [1] K. Sen and M. L. Sen, Introduction to FACTS Controller: Theory, Modeling, and Applications. IEEE Press and John Wiley & Sons, Inc., 2009.
- [2] B. Mork, F. Gonzalez, D. Ishchenko, D. Stuehm, and J. Mitra, "Hybrid Transformer Model for Transient Simulation – Part I: Development and Parameters," IEEE Transactions Power Delivery, vol. 22, no. 1, pp. 248-255, Jan. 2007.
- [3] X. Lin, A. Gole, and M. Yu, "A Wide-Band Multi-Port System Equivalent for Real-Time Digital Power System Simulators," IEEE Transactions on Power Systems, vol. 24, no. 1, pp. 237-249, Feb. 2009.
- [4] K. K. Sen, and M. L. Sen, "Introducing the Family of 'Sen' Transformers: A Set of Power Flow Controlling Transformers," IEEE Transactions Power Delivery, vol. 18, no. 1, pp. 149–157, Jan. 2003.
- [5] M. O. Faruque, and V. Dinavahi, "A Tap-Changing Algorithm for the Implementation of 'Sen' Transformer," IEEE Transactions Power Delivery, vol. 22, no. 3, pp. 1750-1757, Jul. 2007.
- [6] B. Asghari, M. Faruque, and V. Dinavahi, "Detailed Real-Time Transient Model of the 'Sen' Transformer," IEEE Transactions on Power Delivery, vol. 23, no. 3, pp. 1513-1521, July 2008.
- [7] H. Saadat, Power System Analysis, 2nd ed. Boston: McGraw-Hill, 2002.
- [8] G. Slemon, Magnetolectric Devices Transducers, Transformers, and Machines. New York: John Wiley and Sons, Inc., 1966.
- [9] B. Mork, D. Ishchenko, F. Gonzalez, and S. Cho, "Parameter Estimation Methods for Five-Limb Magnetic Core Model," IEEE Transactions Power Delivery, vol. 23, no. 4, pp. 2025-2032, Oct. 2008.
- [10] G. W. Swift, "Power Transformer Core Behavior Under Transient Conditions," IEEE Transactions on Power Apparatus and Systems, vol. PAS-90, no.5, pp. 2206-2210, Sept. 1971.
- [11] S. D. Cho, "Parameter Estimation for Transformer Modeling," PhD thesis, Elec. Comp. Eng., Michigan Tech. Univ., Houghton, USA, 2002.
- [12] AK Steel product data bulletin, "Selection of Electrical Steels for Magnetic Cores," West Chester, OH, 2007.
- [13] H. W. Dommel, Electromagnetic Transients Program Reference Manual (EMTP Theory Book), Portland, OR: Prepared for BPA, Aug. 1986.
- [14] H. Hoidalén, B. Mork, F. Gonzalez, D. Ishchenko, and Nicola Chiesa, "Implementation and verification of the Hybrid Transformer model in ATPDraw," Electric Power Systems Research, vol. 79, no. 3, pp. 454-459, 2009. Special Issue: Papers from the International Conference on Power System Transients (IPST), Lyon, France, Jun. 2007.
- [15] M. N. O. Sadiku, "A Simple Introduction to Finite Element Analysis of Electromagnetic Problems," IEEE Transactions on Education, vol. 32, no. 2, pp. 85-93, May 1989.
- [16] Volume 1 Flux 10 User's Guide– General Tools, Geometry and Mesh, Cedrat, France, 2007.
- [17] H. William Jr. and J. A. Buck, Engineering Electromagnetics, 6th ed. New York: McGraw-Hill, Inc., 2001.
- [18] Volume 2 Flux 10 User's Guide – Physical Description, Circuit Coupling, Kinematic Coupling, Cedrat France, 2007.
- [19] Volume 3 Flux 10 User's Guide – Physical Applications: Magnetic, Electric, Thermal, Cedrat, France, 2007.
- [20] J. C. G. Alonso, "Modeling of Magnetic Non-Linear Characteristics in Electric Machines," MSc. thesis, Dept. of Elec. and Comp. Eng., Univ. of Manitoba, Winnipeg, Canada, 2005.